High-energy astrophysics on compact objects Accretion on all scales

Vieyro F.L.[1,2]

[1] *Instituto Argentino de Radioastronomía (IAR, CCT La Plata, CONICET; CICPBA), C.C.5, (1984) Villa Elisa, Buenos Aires, Argentina*
[2] *Facultad de Ciencias Astronómicas y Geofísicas, Universidad Nacional de La Plata, Paseo del Bosque s/n, 1900, La Plata, Argentina*

Contact / fvieyro@iar-conicet.gov.ar

Resumen / La emisión gamma es la evidencia mas fuerte de que procesos no-térmicos tienen lugar en una fuente astrofísica. Estos procesos son el resultado de la presencia de partículas relativistas que interaccionan con los diferentes campos, como el campo magnético, de radiación y de materia fría. En este trabajo, se describirán los principales procesos radiativos que las partículas sufren en ambientes extremos, que dan lugar a que gran parte de la emisión se produzca en altas energías. Se presentará la fenomenología asociada a las diferentes clases de fuentes con objetos compactos, con particular interés en aquellas sustentadas por la acreción sobre agujeros negros. Finalmente se discutirán algunos de los problemas abiertos asociados a estas fuentes.

Abstract / Gamma-ray emission is the ultimate evidence that non-thermal processes are taking place in an astrophysical source. These processes are the result of the presence of relativistic particles interacting with different fields, such as magnetic, radiation or cold matter fields. In this article, I describe the main radiative processes that particles undergo in extreme environments, that result in a significant fraction of the total emitted power to be released in the gamma-domain. I present the phenomenology related to the different classes of high-energy sources involving compact objects, with particular interest in those powered by accretion into black holes. Finally, I discuss some of the open questions associated with these sources.

Keywords / Radiation mechanisms: non-thermal — Gamma rays: general — Stars: black holes

1. Introduction

The detection and study of gamma ray radiation allows us to explore the properties of the most extreme astrophysical sources in the Universe. Gamma-ray emission is the result of the presence of a populations of relativistic particles accelerated in energetic astrophysical scenarios. The interaction of these relativistic particles with their environment –magnetic field, radiation and cold gas– result in non-thermal emission at high energies.

Some of the sources found to be gamma-ray emitters, in particular some of the most energetic phenomena in the Universe, are powered by accretion onto black holes. The accretion process of matter onto compact objects is the most efficient mechanism know until date to convert rest mass energy into radiation. These include Active Galactic Nuclei (AGNs), which are the result of accretion onto supermassive black holes in the core of galaxies; in a smaller spatial scale, we find the X-ray binaries, which are powered by the accretion onto a compact object -stellar black hole or neutron star- in binary systems.

Although these phenomena can be described by the same basic ingredient of matter accretion (Mirabel & Rodríguez, 1999), the microphysics of these systems might differ. This is why the study of accretion on all scale –both spatial and temporal– can give us information in different astrophysical aspects.

This article is organized as follow: First, in Sec. 2., a description of solutions for different accretion regimes is presented. Then, in Sec. 3. we present the phenomenology observed in accreting stellar lack holes. In Sec. 4. we discuss some open problems associated with different classes of AGNs, and some similarities found between AGNs and XRBs. We conclude with some final remarks in Sec. 5. The relevant non-thermal processes that takes place in gamma-ray sources are briefly described in the Appendix.

2. Accretion flow models

In steady state, the structure of an accretion disk is determined by the mass and spin of the black hole, and by the accretion rate. The latter is usually written in units of the Eddington accretion rate, $\dot{M}_{\rm Edd} = 1.8 \times 10^{-8} M/M_{\odot}$, since sources with similar fraction of the Eddington luminosity are observed to present similar accretion flows (Done et al., 2007).

The structure of the accretion flows is determined by a set of conservation equations (mass, radial momentum, angular momentum and energy), and identifying the processes of heating and cooling of the gas, relevant in each regime (for a more complete discussion and de-

scription on accretion disk models the reader is referred to reviews such as Abramowicz & Fragile 2013).

There are three important solutions of the black hole accretion flows, that are valid for different ranges of accretion rate $\dot{m}$ and optical depth τ: the thin Shakura-Sunyaev disks $\dot{m} \ll 1$, $\tau \gg 1$; the slim disks $\dot{m} \sim 1$, $\tau \gg 1$; and the Advection Dominated Accretion Flow (ADAF) disks $\dot{m} \ll 1$, $\tau \ll 1$.

2.1. Standard disk

The simplest and most popular solution of accretion disk was developed by Shakura & Sunyaev (1973) and Novikov & Thorne (1973). This model, usually know as the standard disk or Shakura-Sunyaev disk, describes the structure of a Keplerian accretion disk around a point mass M. The physical parameters are vertically integrated in this model, hence the solution only depends on the radial coordinate.

In this model, a radial velocity component $v_{\rm r}$ arises as a result of viscous stress, which is responsible of converting gravitational potential into heat, which is radiated locally. The origin of viscosity in accretion disk is now thought to have its origin in the magnetic rotational instability (MRI), which is a self-sustaining dynamo process (Balbus & Hawley, 1991). In the Shakura-Sunyaev disk, however, the stress is treated using a simple approach, in which all viscous effects depends on a simple parameter α, hence the cinematic viscosity ν results in:

$$\nu = \alpha \rho c_{\rm s} h. \tag{1}$$

The solution of Shakura & Sunyaev results in a disk optically thick, that is $\tau > 1$, measured in the vertical direction, and geometrically thin, $H/r \ll 1$. Three regions are found in the solution (see Fig. 1):

- An inner region where the pressure is mainly radiation pressure, and dispersion dominates over absorption.
- A central region where dispersion is still dominant, but the pressure is now dominated by the gas.
- An external region for large r, where the opacity is due to free-free absorption.

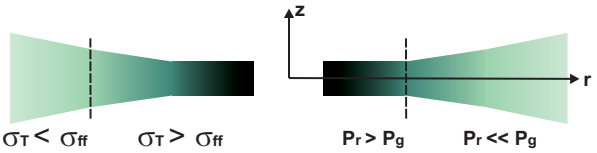

Figure 1: Different disk regions. Here, $\sigma_{\rm T}$ and $\sigma_{\rm ff}$ are the Thomson and free-free cross sections, respectively. Adaptation from Shakura & Sunyaev (1973).

In the external regions, where the disk is optically thick and absorption dominates over dispersion, the disk is in local thermal equilibrium, hence it radiates as a black body with temperature $T(r)$, given by

$$T_{\rm s} = \left\{ \frac{3GM\dot{M}}{8\pi a c r^3} \left[1 - \left(\frac{r_{\rm in}}{r} \right)^{1/2} \right] \right\}^{1/4}. \tag{2}$$

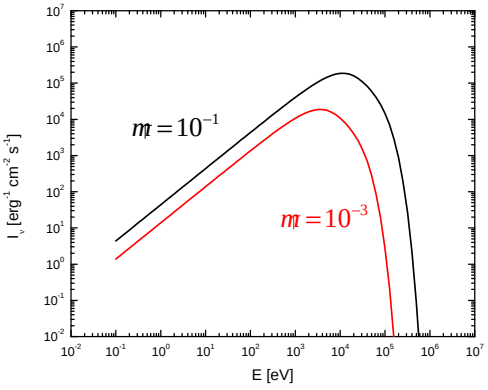

Figure 2: Standard disk spectra. The intensity scale is arbitrary and the accretion rate is in units of $\dot{M}_{\rm Edd}$.

The spectrum is obtained integrating along the disk,

$$I_\nu = 4\pi \int_{r_{\rm in}}^{r_{\rm ext}} F_\nu[T_{\rm s}(r)] r dr. \tag{3}$$

For a local black body spectrum, and a temperature profile given by Eq. 2, a dependence of $I_\nu \propto \nu^{1/3}$ is obtained. Figure 2 shows the spectra of a Shakura-Sunyaev disk around a solar mass black hole, for two values of the accretion rate $\dot{m}$, where $\dot{m} = \dot{M}/\dot{M}_{\rm Edd}$. The spectra peak beyond keV energies, meaning that the disk around an stellar black hole is able to emit soft X-ray photons.

The disk is subject to two instabilities: a thermal instability related to the ionization of hydrogen, which is responsible for the states transitions observed in some XRBs, and an instability due to the radiation pressure (Lightman & Eardley, 1974; Done et al., 2007).

2.2. Slim disk

As in the Shakura-Sunyaev model, this solution assumes that the disk is radiatively efficient. However, at higher accretion rates, advection should be considered as an additional cooling term, and the problem can no longer be solved analytically. The advection modifies the spectrum: for high accretion rates, a large fraction of the heat is advected into the black hole, hence the efficiency of the disk decreases and the disks are only moderately luminous (Abramowicz & Fragile, 2013).

2.3. Hot accretion flows: ADAF

Solutions of thin disks are valid as long as the radiative mechanism is efficient with respect to the local energy dissipation rate; for cases where this is not valid, the structure could result in a geometrically thick disk where $H/r \sim 1$. This is the case of the solutions known as advection dominated accretion flows (e.g., Ichimaru, 1977; Narayan & Yi, 1994, 1995a,b; Abramowicz et al., 1995).

These solutions are valid for sub-Eddington accretion rates ($\dot{m} \ll 1$), where the gas is not dense, hence

the cooling time is longer than the accretion time. The energy released by viscosity is stored as thermal energy in the gas and advected. The plasma results optically thin, and with two temperature (e.g., Yuan & Narayan, 2014).

In the ADAF solutions the radiation pressure is negligible; the two significant contributions to pressure are the magnetic and gas pressure. A second condition is that the interaction between electrons and ions is only through Coulomb interactions and, given the low densities, it is inefficient, and the plasma adopts a two-temperature configuration, with ions much hotter than electrons. Since the energy transfer to electrons is inefficient, and radiation is mainly via electrons, the luminosities of ADAF are lower than the standard disk. Finally, the viscosity is treated as in the Shakura-Sunyaev model, with the parameter α.

Some of the main characteristics of the ADAF solutions are the following:

- the radial velocity is comparable to the free fall velocity;
- the tangential velocity component is sub-Keplerian;
- since cooling is inefficient, the heat is stored as internal energy, the plasma reaches high temperature, causing an elevation of the gas, with a mean height scale $H \sim r$;
- the electrons reach temperatures of $T_e \sim 10^9 - 10^{10}$ K, for $r < 10^3 r_{\rm g}$;
- a significant fraction of the energy is advected, hence the luminosity of ADAF is low.

2.4. Other solutions

Several other solutions have been developed relaxing some of the conditions imposed by the ADAF model, for example:

- ADIOS: adiabatic inflow-outflow solutions (Blandford & Begelman, 1999; Turolla & Dullemond, 2000). This solutions contemplates the possibility that a fraction of the accreted gas is ejected in wind or jets.
- CDAF: convection dominated accretion flows (Quataert & Gruzinov, 2000; Abramowicz & Igumenshchev, 2001). In this model convective instabilities transport angular momentum to inner regions, and the transport of angular momentum outward by other mechanisms is weak.
- LHAF: Luminous hot accretion flows (Yuan, 2001). In this case, the cooling rate of protons for Coulomb interactions is higher than the heating by viscous effects, and the advective term results in heating. This solution is valid for higher accretion rates than those of the ADAF, and results in more luminous and hotter flows.

3. X-ray binaries

X-ray binaries (XRBs) are systems composed by a compact object (a stellar black hole or a neutron star), that accretes material from a companion star. The accretion disk formed in these sources radiates a high fraction of the energy on the X-rays, hence the name of the systems. XRBs are often observed in different spectral states, the most canonical ones being the *high* state and the *low* state. In these states, the X-ray spectrum usually presents two main components: a thermal and a non-thermal component. The thermal component is associated with the emission of a thin standard disk, with an extended black body spectra, whereas the non-thermal component is evidence of a geometrically thick and hot flow, which could be an ADAF, or a component usually known as a *corona* (Stern et al., 2001; Poutanen & Vurm, 2009; Poutanen, 1998; Poutanen et al., 1997). The power-law component is the result of Comptonization of soft photons from the disk by this hot flow.

The phenomenology of the states is the following:

- *High-soft* (HS) state
  The X-ray spectrum in this state is dominated by the thermal component, with a characteristic temperature of $kT \sim 0.7 - 1.5$ keV. The power law is soft, with an index of $\alpha \sim 2.1 - 4.8$ and low intensity. Figure 3 shows the spectra of several sources in this state.
  This state occurs for high accretion rates, $0.09 < \dot{m}$, where the accretion disk can be described by an optically thick Shakura-Sunyaev solution (Esin et al., 1997).

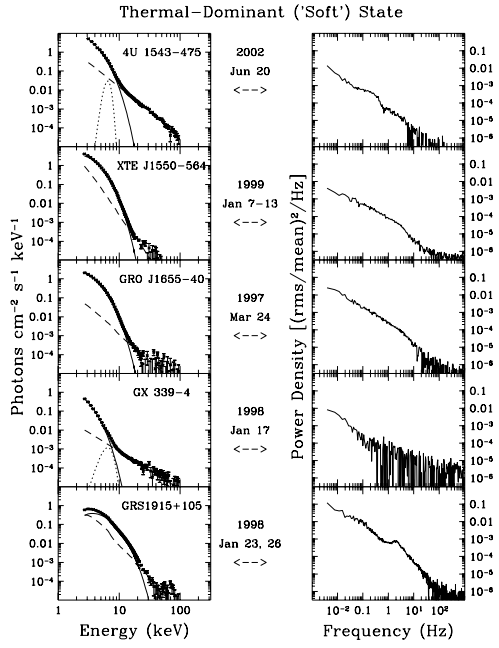

Figure 3: XRBs spectra in the HS state. From McClintock & Remillard (2006).

- *Low-hard* (LH) state
  This state takes place for lower accretion rates, $10^{-2} < \dot{m} < 0.08$, where the geometry of the accretion flow becomes similar to an ADAF in the inner regions, hence the spectra is dominated by the

non-thermal component. The thermal component if shifted towards lower energies, $kT < 0.8$ keV, since the standard disk is truncated at larger radii. Figure 3 shows several examples of the LH state.
Sources that spend a long period in this state are associated with radio emission, which is attributed to the presence of a relativist jet. In these cases the systems are known as *microquasars* (Mirabel et al., 1992). In some sources, as the well studied microquasar Cygnus X-1, VLBI has allowed to resolved the structure of the jet (Stirling et al., 2001).

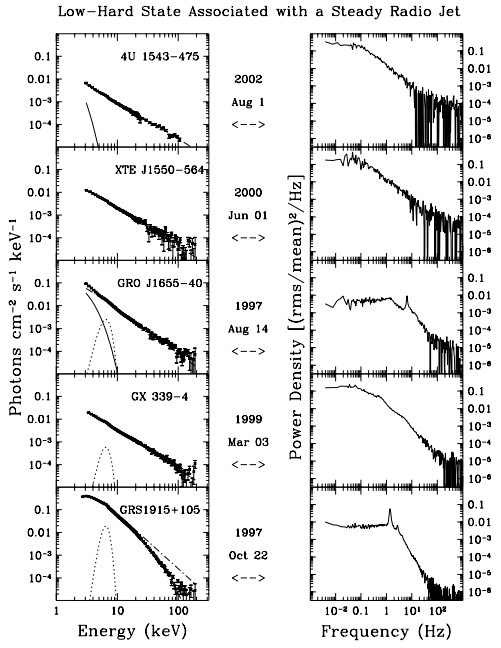

Figure 4: XRBs spectra in the LH state. From McClintock & Remillard (2006).

- *Quiescent* state
  XRBs spent most of their life in a quiescence state, with very low accretion rates $\dot{m} < 10^{-2}$, and ADAF type accretion regime. The spectra during the period of inactivity is similar to the LH state, but with lower luminosities.

3.1. Jets and the dynamical cycle

As mentioned above, the LH state is associated with the presence of steady jets. In addition, state transitions also show radio activity, but in this case the ejections are discrete, more luminous and with higher Lorentz factor than those observed in the LH state.

Fender et al. (2004) proposed a model to describe the dynamical cycle or outbursts that XRB might undergo. In a first phase, and at very low accretion rates, the source is in a low luminous state which correspond to quiescence. When the source enters an activity period,

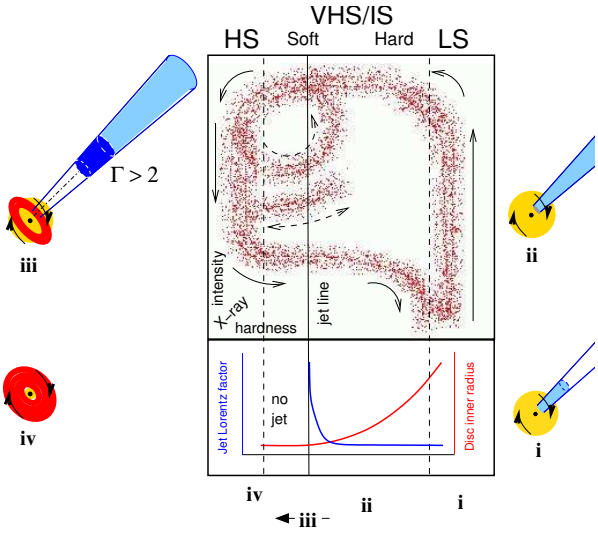

Figure 5: Dynamical cycle in XRBs. From (Fender et al., 2004).

it moves vertically on the diagram towards the LH state, where it shows persistent jets with Lorentz factor mildly relativistic. In the transition from the LH to the HS state, powerful and relativistic jets are launched, which can be the result of the ejection of the inner accretion flow. The disk extends up to the last stable orbit, and the source is in the HS state. During this phase no radio emission is observed. The accretion rate decreases, and the source returns to the quiescent state. Figure 5 shows the diagram of the model, where the solid line marks the cycle.

3.2. Gamma-ray emission from microquasars

Microquasars are known to be variable gamma-ray sources. At least five source are known to emit MeV gamma-rays (McConnell et al., 2000; Cadolle Bel et al., 2006; Paredes & Bordas, 2019), and three of them are also GeV emitters. The MeV emission is found to be polarized, showing a very likely jet origin (Laurent et al., 2011; Jourdain et al., 2012; Zdziarski et al., 2014; Pepe et al., 2015). Alternative models where this emission is originated in a hot accretion flow have also been proposed (Vieyro & Romero, 2012; Romero et al., 2014; Vieyro et al., 2016). The GeV emission is found to be originated far from the compact object, also favoring jet models (Bosch-Ramon, 2007; Zanin et al., 2016).

In the TeV energy range, there was only a 4σ detection of Cygnus X-1 by the MAGIC Collaboration (Albert et al., 2007), by it needs to be confirmed by a higher significance detection. Hence if microquasars

are TeV emitter is still an open question.

4. Accretion onto supermassive black holes

Active galactic nuclei (AGN) are composed of a supermassive black hole that accretes material from the inner region of the galaxy host. Their emission –both thermal and non-thermal– covers the full electromagnetic spectrum, from radio to gamma-rays (see the example in Fig. 6). They present a rich phenomenology, with sources such as Seyfert galaxies, quasars, blazars, radiogalaxies, among others (see, e.g., Padovani et al. 2017 for a detailed review on these sources).

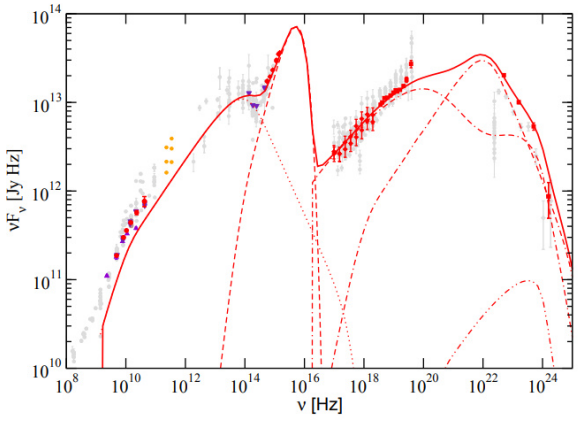

Figure 6: Spectral energy distribution of the blazar 3C 273. The solid line corresponds to a leptonic model, in which the low energy component is synchrotron emission, and the high-energy components are due to inverse Compton interactions. The dashed line is the contribution of the accretion disk. In hadronic models, $p\gamma$ emission and synchrotron of protons can also contribute significantly to the high energy component. From Böttcher et al. (2013).

According to their radiowavelength activity, they can be classified in two main groups: radio-loud and radio-quiet. Since the radio emission is dominated by leptonic synchrotron radiation of the relativistic jet (see the Appendix for a description of the main non-thermal processes), this rough classification is an indicator of the jet power. Within the radio-loud AGNs, the most currently accepted classification system is based principally in three characteristics (Urry & Padovani, 1995): the inclination angle of the jet with the line of sight, the optical spectrum and the radio emission. These AGNs are mainly classified in two groups: blazars, where the jet is almost parallel to the line of sight, hence its luminosity is enhanced by Doppler boosting effects, and radio-galaxies, with large inclination angles, and beaming effects negligible.

The third *Fermi* catalog includes 1591 AGNs, which represents a 71% increment of source in only two years (Ackermann et al., 2015). The 98% of these sources are blazars. However the new generation of Cherenkov instruments has allowed the identification of new classes of AGNs that emit very high-energy (VHE) radiation. In 2009, VHE emission was detected from Seyfert galaxies, in particular Narrow-Line Seyfert 1 (NLS1, Abdo et al. 2009), showing that relativistic jets can be present in AGNs with galaxy host of relatively low mass. The power of these jets is lower than those associated with blazars. This has open new questions in the identification of AGN classes with different evolutionary state in their galaxy hosts in which the classification system of Urry & Padovani was based (Falcke et al., 2004; McHardy et al., 2006; Romero et al., 2017). In addition, this is a problem involving more AGN classes besides NLS1, since *Fermi* surveys show evidence of the existence of other type of AGN with jets, where both the galaxy host and the central black hole have low mass. The detailed classification of AGNs is, thus, being revised continuously, and there are many efforts to replace a purely phenomenological classification by one based on the underlying physics of these complex sources (see, e.g., Foschini 2017 for a more complete discussion).

Regarding the relation between the mass of the central black hole, the AGN activity, and the nature of the galaxy host, there is growing evidence that supports the idea that AGN play a fundamental role in the evolution of its galaxy host (Fabian, 2012). The outflows (both winds and jets) associated with the active nucleus regulate the stellar formation in the galaxy host, effect known as AGN feedback. It is then fundamental to have a more comprehensive view on the properties of different AGN host, to understand the role of feedback on the galaxy evolution, and more generally, on the cosmological evolution (Croton et al., 2006; Bower et al., 2006; McCarthy et al., 2010; Fabian, 2012).

The problems for studying AGNs in different epochs of their evolution are the long timescales involved. For a simple scaling of $\Delta t \propto M_{\rm BH}$, what lasts a fraction of a year for a $10 M_\odot$ black hole, it could last $\sim 10^7$ yr for a $10^9 M_\odot$ black hole. Assuming that the physics behind the accretion process is scale-invariant, the idea is using XRBs as a tool for studying accretion physics, jet launching mechanism, accretion modes, effects of outflows on their ambient media, etc.

Based on the different kinds of AGNs observed in the Universe, and in the so-called fundamental plane of black hole activity, which is a relation between black hole masses, radio and X-ray luminosities across several decades in magnitude in the black hole mass (Merloni et al., 2003; Falcke et al., 2004), it was suggested that different types of AGNs are equivalent to different spectral states of XRBs (Körding et al., 2006). Radio loudness in AGNs could be simple the parallel of the LH states in XRBs, where a persistent jet is found, whereas radio-quiet quasars could be identified with XRBs in the HS state, where no radio emission is observed (Maccarone et al., 2003).

During the last years new evidence supporting the common accretion states in both XRBs and AGNs (Svoboda et al., 2017; Ruan et al., 2019, e.g.,) has grown. However, there are still many questions that remain to be answered and further research is needed.

5. Final remarks

Multiwavelength studies are fundamental to better understand the underlying physics behind accretion. The evidence so far seems to indicate that the accretion process onto black holes is scale invariant (McHardy et al., 2006). If this is correct, then XRB studies might help us understand different states of supermassive black holes and their role on shaping the Universe.

Acknowledgements: This work was supported by the Argentine Agency CONICET (PIP 2014-00338) and the National Agency for Scientific and Technological Promotion (PICT 2017-0898). The author also acknowledges support from the Spanish Ministerio de Economía y Competitividad (MINECO/FEDER, UE) under grants AYA2013-47447-C3-1-P and AYA2016-76012-C3-1-P with partial support by the European Regional Development Fund (ERDF/FEDER), MDM-2014-0369 of ICCUB (Unidad de Excelencia 'María de Maeztu'), and the Catalan DEC grant 2014 SGR 86.

References

Abdo A. A., et al., 2009, ApJL, 707, L142
Abramowicz M. A., Fragile P. C., 2013, Living Reviews in Relativity, 16, 1
Abramowicz M. A., Igumenshchev I. V., 2001, ApJL, 554, L53
Abramowicz M. A., et al., 1995, ApJL, 438, L37
Ackermann M., et al., 2015, ApJ, 810, 14
Albert J., et al., 2007, ApJ, 665, L51
Atoyan A. M., Dermer C. D., 2003, ApJ, 586, 79
Balbus S. A., Hawley J. F., 1991, ApJ, 376, 214
Begelman M. C., Rudak B., Sikora M., 1990, ApJ, 362, 38
Blandford R. D., Begelman M. C., 1999, MNRAS, 303, L1
Blumenthal G. R., Gould R. J., 1970, Rev. Mod. Phys., 42, 237
Bosch-Ramon V., 2007, Ap&SS, 309, 321
Böttcher M., et al., 2013, ApJ, 768, 54
Bower R. G., et al., 2006, MNRAS, 370, 645
Cadolle Bel M., et al., 2006, A&A, 446, 591
Croton D. J., et al., 2006, MNRAS, 365, 11
Done C., Gierliński M., Kubota A., 2007, A&A Rv, 15, 1
Esin A. A., McClintock J. E., Narayan R., 1997, ApJ, 489, 865
Fabian A. C., 2012, ARA&A, 50, 455
Falcke H., Körding E., Markoff S., 2004, A&A, 414, 895
Fender R. P., Belloni T. M., Gallo E., 2004, MNRAS, 355, 1105
Foschini L., 2017, Frontiers in Astronomy and Space Sciences, 4, 6
Ichimaru S., 1977, ApJ, 214, 840
Jourdain E., Roques J. P., Malzac J., 2012, ApJ, 744, 64
Kelner S. R., Aharonian F. A., Bugayov V. V., 2006, PhRvD, 74, 034018
Körding E. G., Jester S., Fender R., 2006, MNRAS, 372, 1366
Laurent P., et al., 2011, Science, 332, 438
Lightman A. P., Eardley D. M., 1974, ApJL, 187, L1
Maccarone T. J., Gallo E., Fender R., 2003, MNRAS, 345, L19
McCarthy I. G., et al., 2010, MNRAS, 406, 822
McClintock J. E., Remillard R. A., 2006, Black hole binaries. pp 157–213
McConnell M. L., et al., 2000, ApJ, 543, 928
McHardy I. M., et al., 2006, Nature, 444, 730
Merloni A., Heinz S., di Matteo T., 2003, MNRAS, 345, 1057
Mirabel I. F., Rodríguez L. F., 1999, Annual Review of Astronomy and Astrophysics, 37, 409
Mirabel I. F., et al., 1992, Nature, 358, 215
Narayan R., Yi I., 1994, ApJL, 428, L13
Narayan R., Yi I., 1995a, ApJ, 444, 231
Narayan R., Yi I., 1995b, ApJ, 452, 710
Novikov I. D., Thorne K. S., 1973, in C. Dewitt & B. S. Dewitt ed., Black Holes (Les Astres Occlus). pp 343–450
Padovani P., et al., 2017, Astronomy and Astrophysics Review, 25, 2
Paredes J. M., Bordas P., 2019, [2019arXiv190209898P], p. arXiv:1902.09898
Pepe C., Vila G. S., Romero G. E., 2015, A&A, 584, A95
Poutanen J., Vurm I., 2009, ApJL, 690, L97
Poutanen J., Krolik J. H., Ryde F., 1997, MNRAS, 292, L21
Poutanen J., 1998, in Abramowicz M. A., Bjornsson G., Pringle J. E., eds., Cambridge Contemporary Astrophysics, Theory of Black Hole Accretion Disks. Cambridge University Press, Cambridge, UK, p. 100
Quataert E., Gruzinov A., 2000, ApJ, 539, 809
Romero G. E., Vieyro F. L., Chaty S., 2014, A&A, 562, L7
Romero G. E., et al., 2017, SSRv, 207, 5
Ruan J. J., et al., 2019, [2019arXiv190302553R]
Shakura N. I., Sunyaev R. A., 1973, A&A, 24, 337
Stecker F. W., 1973, Ap&SS, 20, 47
Stern B. E., Beloborodov A. M., Poutanen J., 2001, ApJ, 555, 829
Stirling A. M., et al., 2001, MNRAS, 327, 1273
Svoboda J., Guainazzi M., Merloni A., 2017, A&A, 603, A127
Turolla R., Dullemond C. P., 2000, ApJL, 531, L49
Urry C. M., Padovani P., 1995, PASP, 107, 803
Vieyro F. L., Romero G. E., 2012, A&A, 542, A7
Vieyro F. L., Romero G. E., Chaty S., 2016, A&A, 587, A63
Yuan F., Narayan R., 2014, Annual Review of Astronomy and Astrophysics, 52, 529
Yuan F., 2001, MNRAS, 324, 119
Zanin R., et al., 2016, A&A, 596, A55
Zdziarski A. A., et al., 2014, MNRAS, 442, 3243

Appendix A:Non-thermal processes

A.1.Leptonic processes

There are two main non-thermal processes of relativistic electrons with the different fields in the source: synchrotron radiation, and inverse Compton (IC) scattering. For sources with a high cold matter density, relativistic Bremsstrahlung could be also relevant.

The synchrotron radiation of ultra-relativistic electrons dominates much of the high-energy astrophysics. One of the general features of the radiation of relativistic electrons is that the radiation is beamed in the direction of motion of the electron. The synchrotron cooling rate for a particle of mass m, charge e, and energy E in a region of magnetic energy density U_B is

$$t_{\rm synchr}^{-1} = \frac{4}{3}\left(\frac{m_e}{m}\right)^3 \frac{c\sigma_T U_B}{m_e c^2}\frac{E}{mc^2}. \quad (A.1)$$

Expressions to calculate the synchrotron spectrum can be found, for example, in Blumenthal & Gould (1970). The power radiated by a single particle of energy E and pitch angle α is given by

$$P_{\rm synchr}(E, E_\gamma) = \frac{\sqrt{3}e^3 B\sin\alpha}{hmc^2}\frac{E_\gamma}{E_{\rm c}}\int_{E_\gamma/E_c}^{\infty} K_{5/3}(\xi)d\xi, \quad (A.2)$$

where $K_{5/3}(\xi)$ is a modified Bessel function and the characteristic energy is

$$E_{\rm c} = \frac{3}{4\pi}\frac{ehB\sin\alpha}{mc}\left(\frac{E}{mc^2}\right)^2. \quad (A.3)$$

For a particle distribution with a power-law spectrum, i.e., $N(E) \propto E^{-\alpha}$, the synchrotron spectrum results in

$$L_\gamma(E_\gamma) \propto E_\gamma^{-\frac{\alpha-1}{2}}, \quad (A.4)$$

which is also a power-law spectrum.

In both Thomson and Klein-Nishina regimes, the IC cooling rate for an electron is given by (Blumenthal & Gould, 1970)

$$t_{\rm IC}^{-1} = \frac{1}{E_e}\int_{\epsilon_{\rm min}}^{\epsilon_{\rm max}}\int_{\epsilon}^{\frac{\Gamma E_e}{1+\Gamma}}(\epsilon_1-\epsilon)\frac{dN}{dtd\epsilon_1}d\epsilon_1. \quad (A.5)$$

Here ϵ is the energy of the incident photon, ϵ_1 is the energy of the scattered photon, and

$$\frac{dN}{dtd\epsilon_1} = \frac{2\pi r_0^2 m_e^2 c^5}{E_e^2}\frac{n_{\rm ph}(\epsilon)d\epsilon}{\epsilon}F(q), \quad (A.6)$$

where $n_{\rm ph}(\epsilon)$ is the density of target photons, r_0 the classical radius of the electron, and

$$\begin{aligned} F(q) &= 2q\ln q + (1+2q)(1-q) + \frac{1}{2}(1-q)\frac{(\Gamma q)^2}{1+\Gamma q}, \\ \Gamma &= 4\epsilon E_e/(m_e c^2)^2, \\ q &= \epsilon_1/[\Gamma(E_e-\epsilon_1)]. \end{aligned} \quad (A.7)$$

According to Blumenthal & Gould (1970), the spectrum of photons scattered by an electron of energy $E_e = \gamma_e m_e c^2$ in a target radiation field of density $n_{\rm ph}(\epsilon)$ is

$$P_{\rm IC}(E_e, E_\gamma, \epsilon) = \frac{3\sigma_{\rm T} c (m_e c^2)^2}{4E_e^2}\frac{n_{\rm ph}(\epsilon)}{\epsilon}F(q), \quad (A.8)$$

where $F(q)$, q, and Γ are given by Eq. (A.7) (in this case $\epsilon_1 = E_\gamma$). The allowed range of energies for the scattered photons is

$$\epsilon \leq E_\gamma \leq \frac{\Gamma}{1+\Gamma}E_e\ . \quad (A.9)$$

The total luminosity can then be obtained from

$$L_{\rm IC}(E_\gamma) = E_\gamma^2\int_{V_{\rm c}} d^3r \int_{E_{\rm min}}^{E_{\rm max}} dE_e\ \ N_e(E_e) \times \int_{\epsilon_{\rm min}}^{\epsilon_{\rm max}} d\epsilon P_{\rm IC}(\quad (A.10)$$

This equation takes into account the Klein-Nishina effect on the cross-section with energy.

A.2.Hadronic processes

For sources where an hadronic component can also be accelerated up to relativistic energies, the main hadronic processes for gamma emission are synchrotron radiation, photohadronic interactions and proton-proton inelastic collisions in some cases. Hadronic interactions produce neutral pions, which have a short mean lifetime of 8.4×10^{-17} s, and then they decay with a probability of 98.8 % into two gamma rays

$$\pi^0 \rightarrow \gamma + \gamma. \quad (A.11)$$

The photomeson production takes place for photon energies above $\epsilon_{\rm th} \approx 145$ MeV (measured in the rest-frame of the proton). Near the threshold, a single pion is produced per interaction; at higher energies, the production of multiple pions dominates.

The cooling rate due to photopion production for a proton of energy E_p in an isotropic photon field of density $n_{\rm ph}(\epsilon)$ is given by (Stecker, 1973)

$$t_{p\gamma}^{-1}(E_p) = \frac{m_p^2 c^5}{2E_p^2}\int_{\frac{\epsilon_{\rm th}}{2\gamma_p}}^{\infty} d\epsilon \frac{n_{\rm ph}(\epsilon)}{\epsilon^2}\int_{\epsilon_{\rm th}}^{2\epsilon\gamma_p} d\epsilon' \sigma_{p\gamma}(\epsilon')K_{p\gamma}(\epsilon')\epsilon', \quad (A.12)$$

where ϵ' is the photon energy in the rest-frame of the proton and $K_{p\gamma}$ is the inelasticity of the interaction. Atoyan & Dermer (2003) introduced a simplified approach to treat the cross-section and the inelasticity, which can be written as

$$\sigma_{p\gamma}(\epsilon') \approx \begin{cases} 340\ \mu{\rm barn} & 200{\rm MeV} \leq \epsilon' \leq 500{\rm MeV} \\ 120\ \mu{\rm barn} & \epsilon' \geq 500{\rm MeV}, \end{cases}$$

and

$$K_{p\gamma}(\epsilon') \approx \begin{cases} 0.2 & 200{\rm MeV} \leq \epsilon' \leq 500{\rm MeV} \\ 0.6 & \epsilon' \geq 500{\rm MeV}. \end{cases}$$

At energies below the threshold for photomeson production, the main channel of proton-photon interaction is the direct production of electrons or positrons. The cooling rate is also given by Eq. (A.12), and the corresponding cross-section and inelasticity. The cross-section for this channel - also known as the Bethe-Heitler cross-section- increases with the energy of the photon. Both the cross-section and inelasticity approximations in the limits of low and high energies can be found in Begelman et al. (1990).

The cooling rate for inelastic collisions of protons with nuclei of the source is given by:

$$t_{pp}^{-1} = n_i c \sigma_{pp} K_{pp}, \quad (A.13)$$

where n_i is the cold matter density, K_{pp} is the total inelasticity of the process, of value ~ 0.5. The total cross-section σ_{pp} can be approximated by (Kelner et al., 2006)

$$\sigma_{\rm inel}(E_p) = (34.3{+}1.88L{+}0.25L^2)\left[1-\left(\frac{E_{\rm th}}{E_p}\right)^4\right]^2, \quad (A.14)$$

where

$$L = \ln\left(\frac{E_p}{1\ {\rm TeV}}\right). \quad (A.15)$$

The proton threshold kinetic energy for π^0 production is $E_{\rm th}^{\rm kin} \approx 280$ MeV.